THE JOURNAL OF COMPARATIVE NEUROLOGY 193:187-202 (1980)

Retinotopic Organization of Striate and Extrastriate Visual Cortex in the Mouse

EARL WAGOR, NANCY J. MANGINI AND ALAN L. PEARLMAN
Department of Physiology and Biophysics and Department of Neurology and Neurological Surgery (Neurology), Washington University School of Medicine, St. Louis, Missouri 63110

ABSTRACT Detailed retinotopic maps of primary visual cortex (area 17) and the extrastriate visual regions surrounding it (areas 18a and 18b) have been constructed for the C57BL/6J mouse using standard electrophysiological mapping techniques.

Primary visual cortex (area 17), as defined cytoarchitectonically, contains one complete representation of the contralateral visual field, termed V1, in which azimuth and elevation lines are approximately orthogonal. The upper visual field is represented caudally and the nasal field laterally. Binocular cells are encountered in the cortical representation of the nasal 30–40° of the visual field, and there is an expanded representation of the nasal field.

Extrastriate visual cortex of the mouse, like that of other mammals, contains multiple representations of the visual field. The cytoarchitectonic region of cortex lateral and rostral to area 17, termed area 18a, contains at least two such representations. The more medial of these, which by convention we have called V2, is a narrow strip surrounding V1 on its lateral and rostral aspects; the vertical meridian lies along a portion of its common border with V1. The visual field representation in V2 is not a mirror image of that in V1; the representation of the horizontal meridian forms the lateral border of V2, and the visual field representation is split so that adjacent points on either side of the horizontal meridian are represented in nonadjacent parts of V2. The other visual field representation within area 18a, which we have termed V3, is a small but apparently complete representation that lies lateral to V2. The visual field representations medial to area 17 correspond to cytoarchitectonic area 18b. Area 18b contains two representations of the temporal visual field that we have labeled Vm-r and Vm-c, and contains little or no representation of the most nasal aspect of the field.

Architectonic studies of mammalian cerebral cortex in the early part of this century divided extrastriate visual cortex into two regions, areas 18 and 19, that formed concentric rings surrounding primary visual cortex (area 17) (Brodmann, '05, '09). In recent years a number of observations have indicated the need for revision of this concept (Allman, '77; Kaas, '80; Van Essen, '79; Zeki, '76 for reviews). Cats and primates have many more than two distinct extrastriate visual regions, and their arrangement is considerably more complex than the early cytoarchitectonic studies suggested (Allman and Kaas, '74a,b, '75, '76; Palmer et al., '78; Spatz and Tigges, '72a,b; Tigges et al., '73, '74, Tusa et al., '79; Van Essen and Zeki, '78; Zeki and Sandman, '76; Zeki, '69, '71, '76). Although the role of these cortical regions in vision is at present unclear,

Address reprint requests to Alan L. Pearlman, Washington University School of Medicine, 660 S. Euclid, St. Louis, MO 63110. Earl Wagor's present address is: Gladstone Foundation Cardiovascular Laboratories, P.O. Box 40608, San Francisco, CA 94140. Nancy J. Mangini's present address is: Department of Biological Sciences, Purdue University, West Lafayette, IN 47907.

0021-9967/80/1931-0187$02.90

there is evidence that at least some of the regions may be specialized for particular visual functions (Hubel and Wiesel, '70; Pearlman et al., '79; Zeki, '78).

Several recent studies of mammals other than monkeys and cats suggest the need for a re-evaluation of the classification scheme for cortical visual regions in these animals as well. (Benevento and Ebner, '71; Chow et al., '77; Hall et al., '71; Montero et al., 73a,b; Montero and Murphy, '76; Towns et al., '77; Olavarria and Mendez, '79; Mathers et al., '77; Woolsey et al., '73). The mouse has received particular attention because of its potential usefulness in the correlation of genetic variability with neural function. In addition, the lissencephalic brain of the mouse facilitates the task of determining the retinotopic organization of cortical visual areas.

A number of early reports provide descriptions of the cytoarchitectonic fields in the cerebral cortex of the mouse (Isenschmid, '11; De Vries, '12; Drooglever Fortuyn, '14; Rose '12, '29). More recently, Caviness ('75) has described the architectonic distinctions between cortical areas in the mouse, and has developed a parcellation system similar to that devised for the rat by Krieg ('46a,b, '47). According to Caviness ('75), there are two extrastriate visual regions in the mouse: area 18a, extending posterior, lateral, and anterior to area 17, and area 18b, lying medial to area 17. Drager's ('75) analysis of the receptive field properties of neurons in area 17 of the mouse also provided evidence that these two extrastriate regions contain representations of the visual field and suggested that these are compressed mirror images of the area 17 representation. We undertook the present detailed study of the retinotopic organization of striate and extrastriate visual regions of the mouse in order to provide a framework for studies of these regions in mutant mice. The results have proved to be of interest from a comparative point of view as well, since some of the principles of organization of the visual cortical areas in the mouse are similar to those of the monkey and cat.

METHODS

Detailed retinotopic maps of striate and extrastriate visual areas were constructed from the results obtained in 21 C57BL/6J mice (Jackson Laboratories, Bar Harbor, Maine). The mice, ranging from 8 weeks to 6 months of age, were anesthetized with an initial 0.3-0.4 cc intraperitoneal injection of a 10% solution of urethane (approximately 1.5 g/kg) with supplementary 0.05-0.1 cc doses as needed. We found urethane to be the most suitable anesthetic agent of several we tried. Once surgical anesthesia had been achieved, most mice did not require additional doses for 12–18 hours. A 20% depression in respiratory and heart rates occurred with urethane, compared to a 50% reduction often seen with barbiturate anesthesia. More importantly, there was much less depression of cortical activity evident with urethane than with anesthetic doses of barbiturates. In addition, the clouding of the optics of the eye sometimes associated with barbiturate anesthesia (Fraunfelder and Burns, '70) was not a problem with urethane.

A section of polyethylene tubing was inserted into the trachea so as to maintain a clear airway. The oxygen content of the inspired air was increased by passing a continuous stream of 100% 0_2 through a small glass cup placed over the opening of the tracheal tube. Silicon fluid (Dow Corning) was applied to the corneas to prevent drying. Body temperature was maintained at 37°C with a feedback-controlled heating pad. The mouse was placed in a head holder with ear and incisor bars designed so as not to obstruct the animals's field of vision. The horizontal plane of this holder was parallel to the floor and intersected the intraaural line and a point 3 mm above the incisor bar. A major portion of the parietal bone (approximately 5 mm^2) overlying the posterior aspect of the left hemisphere was removed by drilling along the skull sutures. In this manner, a large area of cortex was exposed with minimal damage to the dura which is closely applied to the cortical surface. The dura was left intact. A petroleum jelly reservoir was constructed around the opening, and filled with warm mineral oil. An enlarged photograph of the exposed brain was used to plot the position of each electrode penetration on the cortex with respect to cortical blood vessels.

Recordings were made with lacquer-coated tungsten microelectrodes that had resistances of $7–8 \times 10^5$ ohms. These electrodes mainly recorded from small clusters of units and occasionally isolated single cells. Receptive field position was defined as the center of the receptive field of the recorded unit cluster. Penetrations were made in rows in either a mediolateral or rostro-caudal direction, depending upon the particular part of visual cortex to be explored. The distance between electrode pen-

etrations in area 17 was usually 0.3–0.5 mm; in extrastriate visual cortex the distance was 0.1–0.2 mm due to the relative compression of the representation of the retina in these regions.

Electrolytic lesions (4 μA for 4 sec) for subsequent histological localization were made during selected electrode penetrations that were thought to be near the border of area 17. At the end of each experiment, the mouse was perfused through the heart with 10% formalin. The brain was frozen and cut either coronally or sagittally in 50 μm serial sections that were stained with thionin.

Eye movements

In the initial stages of these investigations, we obtained unsatisfactory results during attempts to maintain a paralyzed animal in good physiological condition for long periods of time. Therefore, the mice in this study were not paralyzed and no attempt was made to stabilize the eye. In the study by Drager ('75), direct measurements made to test the extent of eye movements in nonparalyzed animals showed that there were no large, rapid eye movements and that slow drifts never exceed 2–3° per hour under barbiturate anesthesia. Cicerone and Green ('77) made direct measurements of the eye movements that occur in rats anesthetized with urethane and reported finding a slow continuous drift of up to 4.5° per hour. This appears not be be the case for mice; we found that when the microelectrode was returned to a given cortical position during the course of 24–48 hour experiment, the visual field position represented by that point never differed by more than 5° from the receptive field position plotted originally. This value is within the range of scatter found among receptive field positions plotted for cells in a single perpendicular penetration. During single-unit isolation experiments, cells with small receptive fields were analyzed for periods of up to 3.5 hours with negligible drift in receptive field position (Mangini and Pearlman, '80).

Visual field mapping

Since there are a number of technical difficulties associated with viewing retinal landmarks in the mouse's eye, we chose to use visual field reference planes related to head position rather than retinal features for identifying receptive field locations. In this system, elevation lines were parallels above (positive values) and below (negative values) the equator (0°) of the hemisphere used for visual field mapping. Receptive fields were plotted on a translucent plastic dome that was a segment of a sphere with a radius of 28.6 cm, positioned so that the animal's right eye was at the center of the sphere. Rectangles and slits of light of varying sizes were projected onto the convex side of the screen with a small tripod-mounted projector. A level and plumb line were used to adjust the hemisphere so that its equator was parallel to the floor and at a height equal to the distance from the center of the mouse's eye to the floor. A series of parallel azimuth lines divided the hemisphere in the naso-temporal dimension (Bishop et al., '62). The 0° azimuth line, or vertical meridian, was defined by the intersection of the midsaggital plane of the head with the hemisphere.

Receptive field positions for each electrode position (as determined by surface micromanipulator readings) were plotted for each experiment. No correction was made for the slight curvature of the cortical surface because the maximum degree of error introduced by the convexity in the areas mapped was calculated to be less than 10%. Isoazimuth and isoelevation lines were then drawn and the resultant map was superimposed on a drawing of the dorsal view of the cerebral hemisphere. The borders of area 17 were drawn with histologically verified lesions as reference points.

RESULTS

Observations were made on 21 mice; in eight of these experiments sufficient data were collected from 535 electrode penetrations to generate detailed retinotopic maps of different portions of area 17 and extrastriate visual cortex. The degree of overlap among the individual maps was sufficient to permit construction of a composite. We will first present the results of individual experiments that map particular segments of striate and extrastriate cortex, and then consider the features of the composite map.

Retinotopic maps

Figure 1 shows one medial to lateral series of penetrations taken from a case in which a large number of penetrations were placed in extrastriate cortex lateral to area 17. Note that as the electrode placement proceeded from medial to laterial (penetrations 1 through 4) the receptive field positions progressed from temporal to nasal. As the penetrations continued in the lateral direction (5 through 7), receptive field positions shifted

back from nasal to temporal. Continuing in the lateral direction (penetrations 8 and 9) resulted in receptive field positions shifting once again from temporal to nasal. A lesion placed at the location of penetration 4, which was the site of the first reversal in receptive field position, demonstrated that this reversal occurred at the cytoarchitectonic 17-18a border.

The series of electrode penetrations shown in Figure 1 was taken from a case in which a total of 91 cortical points were examined. A map of isoelevation and isoazimuth lines for lateral striate and extrastriate visual cortex was constructed from these data and is shown in Figure 2. The noteworthy features of this map include the following: 1) Within area 17, the amount of cortex containing a representation of the nasal visual field between 20° and 40° above the equator is disproportionately large. 2) The lateral border of area 17 corresponds for some distance with the line representing the most nasal extent of the visual field representation, i.e., the 0° isoazimuth line. 3) The isoelevation lines that run in a caudo-medial to rostro-lateral direction in area 17 diverge as they cross the 17-18a border. One group, consisting of lines representing the visual field below +20°, curves rostrally as it crosses the 17-18a border and courses in an antero-medial direction, while a second group, made up the lines representing the visual field above +30°, curves posteriorly and courses in a caudo-lateral direction. Lateral to the two groups of isoelevation lines just described, the organization becomes much more complex. Specific details of this lateral region will be discussed in connection with the composite retinotopic map.

Isoazimuth lines, in contrast to isoelevation lines, follow a fairly straightforward plan of organization in area 17 and lateral extrastriate cortex. Throughout the extent of this map, isoazimuth lines run in an approximately rostro-caudal direction. In area 17, isoazimuth lines representing the temporal field are found medially while those representing the nasal field are located laterally (Figs. 2, 3, 4A). A reversal in this trend occurs at the 17-18a border. In the central part of the lateral extrastriate area there is a second reversal in isoazimuth lines that indicates an additional nasal field representation in the portion of lateral extrastriate cortex representing the lower visual field (Fig. 4A). However, in the zones posterior and anterior to this region such a reversal is not evident; instead, the extreme peripheral fields are represented.

An example of a case in which the anterior and medial aspect of the visual cortex was explored is shown in Figure 3A. The region near the anterior border of area 17 contains a representation of the lower visual field; the representation of the visual field below −40° is confined to cytoarchitectonically defined area 17. It should also be noted that something like the divergence previously described for isoelevation lines in lateral visual cortex occurs here for isoazimuth lines as they cross the antero-medial border of area 17. Isoazimuth lines representing positions more nasal than 70° turn laterally after crossing the border while isoazimuth lines representing positions more temporal than 80° veer sharply to run in a medial direction. The antero-medial border of area 17, as defined histologically, crosses through the points at which these isoazimuth lines abruptly change course (Fig. 3A–D).

Borders of area 17

During the course of most experiments, lesions were made at locations that were thought to be on or near the border of area 17 for subsequent correlation of the anatomically defined visual areas with the retinotopic map. Histological identification of area 17 was based on the cytoarchitectonic criteria outlined by Caviness ('75); in particular, the greater width and cell density of layer IV and the distinctive hypocellular zones of layer V in area 17 relative to area 18a and 18b were useful in making these distinctions.

In the experiment described above (Fig. 3A), in which anterior and medial visual cortex were explored, three lesions were made during electrode penetrations that were in cortex representing the extreme inferior aspect of the visual field and therefore presumed to be near the rostral border of area 17. These three lesions sites are indicated by circles in Figure 3A; they were subsequently identified in serial parasaggital sections. The lesion falling at the rostral border of area 17 is indicated by the star symbol in Figure 3A and is shown in Figure 3B.

A similar retinotopic map for a case in which the medial aspect of area 17 was explored is shown in Figure 3C. Two of the three electrolytic lesions placed in this case fell on the medial border of area 17; the more caudal of these, indicated by a star in Figure 3C, is shown in Figure 3D. The retinotopic map and the lesion locations indicate that the medial

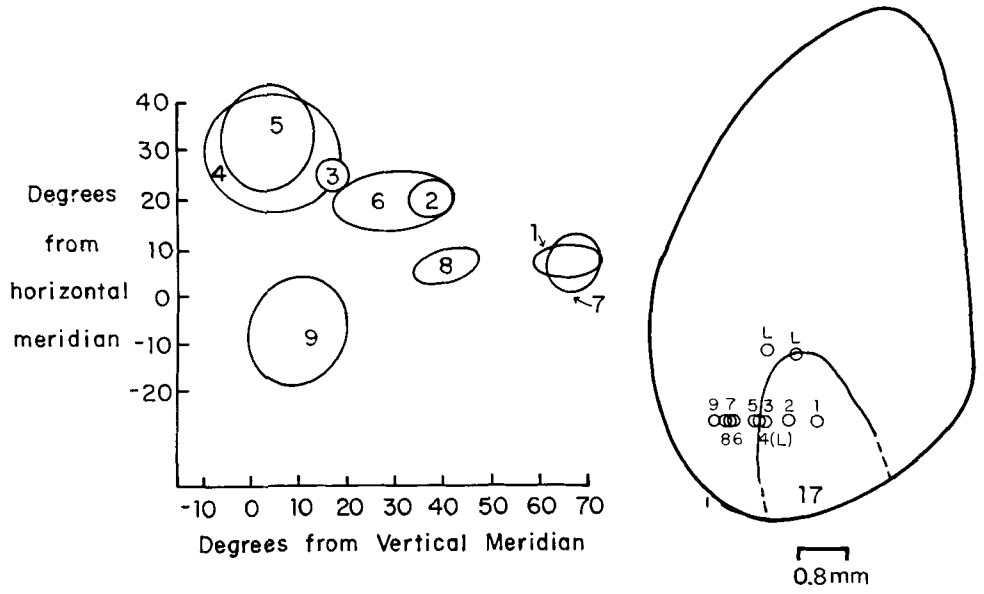

Fig. 1. Receptive field positions, as mapped on the visual field screen during a series of nine electrode penetrations starting in area 17 and progressing in a medial to lateral direction into area 18a. Two reversals in receptive field positions were observed in this series, taken from the case shown in detail in Figure 2. The cytoarchitectonically defined border of area 17 is indicated by the solid line in the dorsal view of the left hemisphere shown on the right. Penetrations containing lesions are indicated by L.

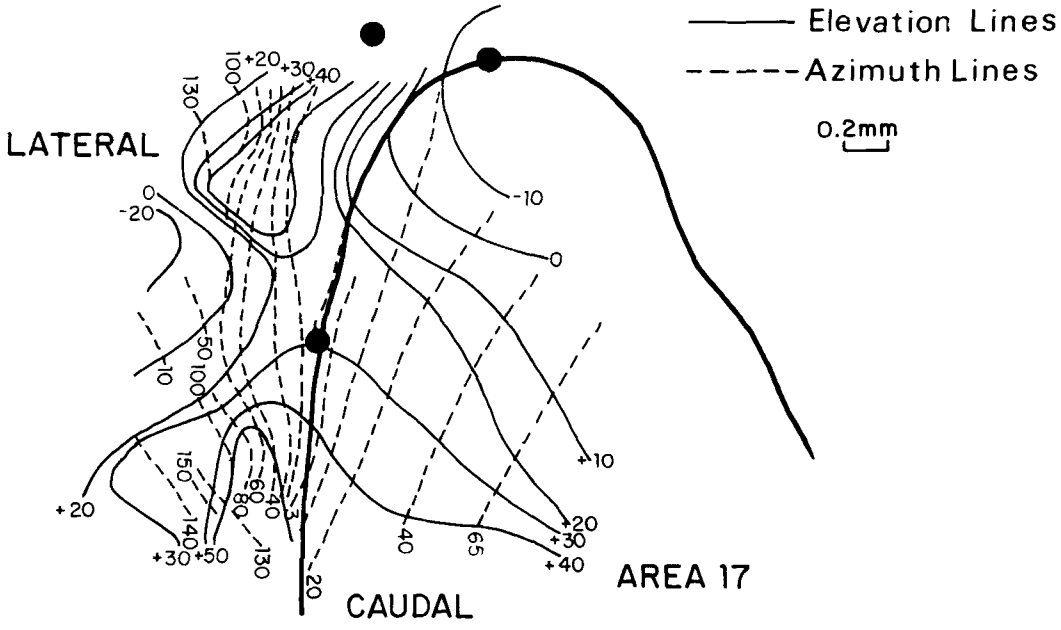

Fig. 2. Topographic map of lateral striate and extrastriate visual cortex constructed from the receptive field positions mapped for 91 cortical electrode penetrations in a single animal. In this map and those following, isoelevation lines indicate receptive field positions above and below the equator of the hemisphere and isoazimuth lines indicate receptive field positions in the naso-temporal dimension. Isoelevation lines are labelled by numbers preceded by + or − signs. Numbers labelling isoazimuth lines are rotated 90°. The heavy solid line indicates the location of the cytoarchitectonically determined area 17 border. Sites of lesions confirmed histologically are shown as filled circles.

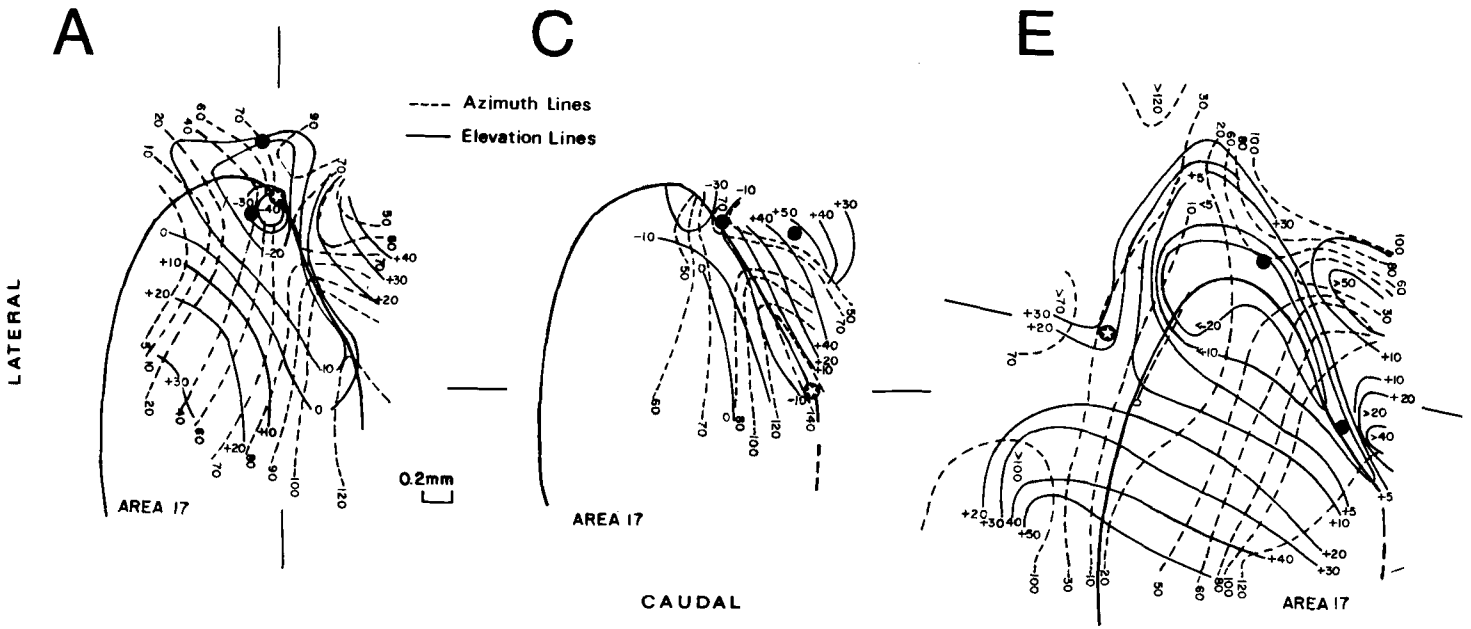
A
C
E
Azimuth Lines
Elevation Lines
LATERAL
CAUDAL
AREA 17
AREA 17
AREA 17
0.2mm

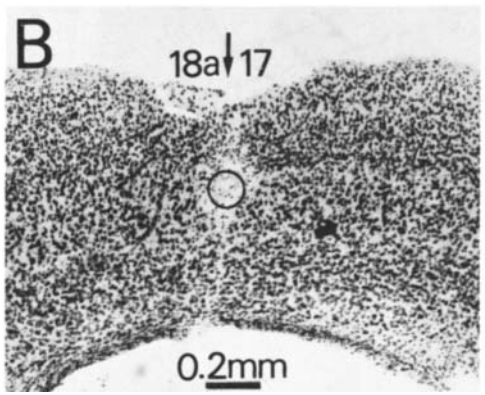
B
18a
17
0.2mm

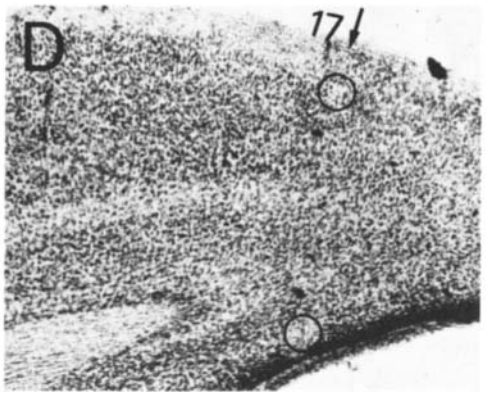
D
17

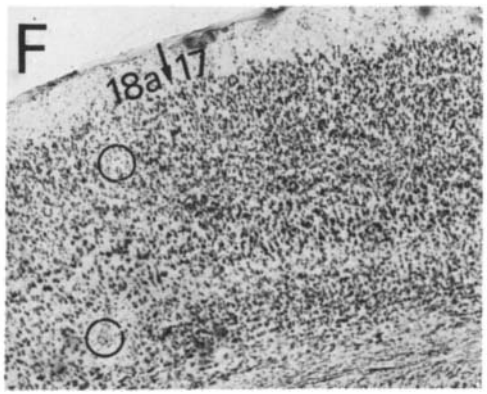
F
18a
17

border of area 17 corresponds to the most temporal aspect of the visual field representation.

The most extensive retinotopic map constructed from the results obtained in a single animal is illustrated in Figure 3E. Since an attempt was made to explore as much of striate and extrastriate cortex as possible during the course of this experiment, the distance between electrode penetrations was of necessity greater than in experiments concentrating on particular subregions of visual cortex. A lesion produced at a cortical recording site just lateral to a penetration where a naso-temporal reversal in receptive field position occurred (Fig. 3E, star) proved to be lateral to the histologically determined border by the appropriate distance (Fig. 3F, upper circle).

A composite retinotopic map

The composite retinotopic map illustrated in Figure 4A was constructed by collating the maps obtained in eight animals. Several features of this map have already been mentioned in dealing with the specific cases; a number of additional points are best considered in relation to the composite.

Area 17 As indicated earlier, striate cortex contains a complete representation of the visual field in which isoazimuth and isoelevation lines are approximately orthogonal. The upper field is represented caudally and the nasal fields laterally. Binocular cells are encountered in the cortical representation of the nasal 30–40° of the visual field (finely stippled area, Fig. 4A). The organization of area 17 in the mouse as described here is generally in agreement with that previously described by Drager ('75), with two exceptions.

First, we find that the nasal visual field has a somewhat expanded representation in area 17. This expansion involves the nasal field between the 0° and 30° isoazimuth lines and between the 0° and +40° isoelevation lines (Fig. 4A). The magnification factor (mm of cortex per degree of visual field) for various points along the +25° isoelevation line in area 17 is shown in Figure 5. The magnification factor near the 0° isoazimuth line is approximately twice that found in the representation of the field temporal to the 30° isoazimuth line.

Second, Drager ('75) reported that the reversal of receptive field position at the lateral border of area 17 occurred when the geometric centers of the receptive fields had progressed for at least 10° into the ipsilateral visual field. She further indicated that the receptive fields of binocular cells were always separated horizontally by about 5–20° in the barbiturate anesthetized mouse, making it necessary to correct for ocular divergence in plotting receptive field positions. In contrast, we found that the reversal seldom occurred ipsilateral to the 0° azimuth line and more often occurred several degrees contralateral to it. In addition, no correction for ocular divergence was necessary in our analysis, since the centers of the receptive fields mapped for binocular units in our recordings were in most cases coincident (Fig. 6). The displacement of receptive field centers that did occur in a few binocular units was not consistently divergent (Fig. 6) and occasionally had a vertical component.

In an experiment specifically devoted to a search for an ipsilateral visual field representation in area 17, we made numerous electrode penetrations in medial-to-lateral rows, exploring the nasal visual field between −20° and +50° elevations. These rows of electrode penetrations are shown in Figure 7a in relation to the cytoarchitectonically determined 17-18a border. Figure 7B shows the progression of receptive field centers toward the vertical meridian as the electrode sampled from medial to lateral in area 17, and the subsequent reversal that occurred by continuing across

Fig. 3. Correlation of physiologically determined V1 borders with anatomically defined 17-18a and 17-18b borders. In the retinotopic maps illustrated in A, C, and E, solid lines represent isoelevation lines and dashed lines represent isoazimuth lines. All maps are of the left cerebral hemisphere seen from above. Circles indicate the location of lesions made during the experiments. Stars indicate the lesions pictured in B, D, and F. The solid lines extending in the rostrocaudal direction in A and medio-lateral direction in C and E indicate the plane of the histological sections illustrated. A. Retinotopic map of anterior and medial visual cortex resulting from 64 penetrations in case M 100. B. Parasaggital section through visual cortex illustrating that the lesion indicated by the star in A is located at the rostral border of area 17. This result demonstrates that the visual field below −40° is confined to area 17. C. Retinotopic map of medial striate and extrastriate visual cortex determined from 63 penetrations in case M 97. The star shows the anatomically defined location of a lesion made where a reversal in receptive field position was noted. D. Coronal section through visual cortex showing that the lesion indicated by the star in C is located at the cytoarchitectonically defined medial border of area 17. E. Retinotopic map encompassing most of visual cortex constructed from the results of 88 relatively widely spaced (0.3–0.4 mm) electrode penetrations. F. Coronal section showing that the lesion denoted by the star in E is located lateral to the cytoarchitectonic 17-18a border. The medial border of 17 is at the right edge of the photograph.

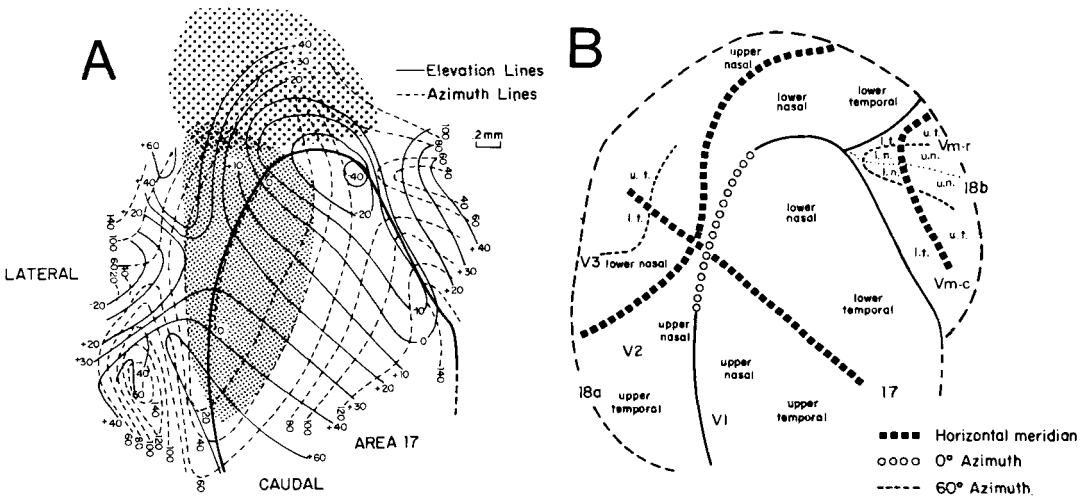

Fig. 4. Composite retinotopic map. A. The organization of isoazimuth and isoelevation lines in this retinotopic map of striate and extrastriate cortex of the left cerebral hemisphere was determined by combining the detailed maps of subregions obtained in eight different animals (see text for detailed description). The finely stippled area indicates the region of cortex where binocular units were encountered. The coarsely stippled region designates the area in which units with both visual and vibrissal responses were encountered. B. Schematic version of the retinotopic map in A, emphasizing those features relevant to the determination of the subdivisions of extrastriate cortex. Abbreviations: u.t., upper temporal; l.n., lower nasal, etc.

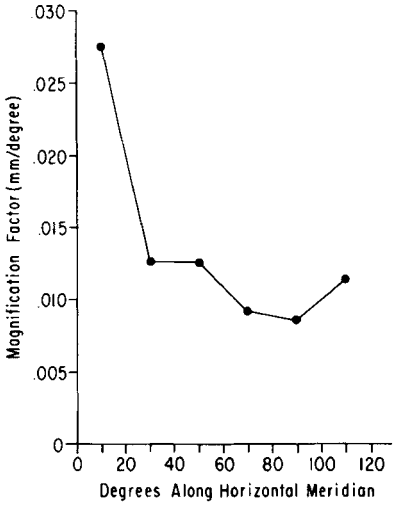

Fig. 5. Magnification factor in mm/degree calculated from the composite retinotopic map (Fig. 4A) for points along the +25° elevation line in area 17. The magnification factor at each point was determined from the composite map by dividing the distance (mm of cortex) between azimuth lines, indicated in 20° intervals, by 20 to give average mm cortex/degree visual field. The value calculated for each 20° segment was then plotted on the graph at the midpoint of each interval.

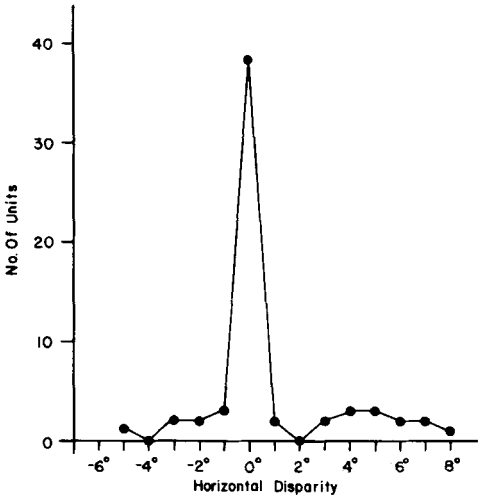

Fig. 6. Horizontal disparity in receptive field positions for 67 binocular units in area 17 in 7 experiments. Negative values indicate that the receptive field plotted by stimulating the ipsilateral eye was temporal to the receptive field obtained by stimulating the contralateral eye.

into lateral extrastriate cortex. The most nasal receptive field encountered in each medial to lateral series of penetrations in this experiment has been plotted in Figure 7C. Although several of these receptive fields extend into the ipsilateral visual field by as much as 20°, none had their geometric centers more than 2–3° into the ipsilateral field.

Since our retinotopic maps, like most others, are constructed to indicate the geometric centers of encountered receptive fields, we have shown little or no progression into the ipsilateral visual field in area 17 on our composite map. The 0° isoazimuth line may be taken as the point of reversal in receptive field positions in the lateral aspect of area 17. As stated earlier, our lesion studies demonstrate that this reversal takes place at the lateral 17-18a border.

Extrastriate Visual Regions The organization of isoazimuth and isoelevation lines in extrastriate visual cortex is much more complex than in area 17, and does not yield a simple mirror image of the map in striate cortex (Fig. 4A). Indeed, at first glance it is not clear how extrastriate cortex should be subdivided into regions containing visual field representations. The situation is clarified somewhat by considering the +25° isoelevation line. (This is the heavy broken line in Figure 4B labeled Horizontal Meridian; for reasons to be dealt with in the Discussion, we consider the +25° elevation line in our coordinate system and the horizontal meridian to be equivalent.) The +25° isoelevation line bisects area 17 into nearly equal upper and lower field representations, and then trifurcates after crossing the 17-18a border (Fig. 4A,B). The posterior extension of the 25° isoelevation line in 18a forms the lateral border of an area containing a representation of the upper visual field, while the anterior leg forms the lateral border for an area containing a representation of the lower visual field (Fig. 4A). These two subareas taken together form one complete visual field representation; by convention (Allman, '77; Van Essen, '79) we have labelled this V2 (Fig. 4B). The region lateral to V2 has the +25° isoelevation line as its medial boundary; it is divided by the lateral extension of the +25° isoelevation line into an anterior subarea representing the upper visual field and a posterior subarea containing a representation of the lower visual field (Fig. 4A). These two regions, taken together, form a third representation of the visual field that we have labelled V3 (Fig. 4B). Thus there are at least two visual field representations, V2 and V3, within the cytoarchitectonically distinct and apparently uniform area 18a.

The division of lateral extrastriate visual cortex into two regions does not take into account two additional partial representations of the visual field. In the extreme posterior aspect of V2, there is a reversal in the progression of isoazimuth lines as one proceeds laterally, yielding a partial reduplication of the upper temporal visual field (Fig. 4A). There is also an indication of a small additional representation of the lower nasal visual field in the extreme posterior aspect of V3 (Fig. 4A). Our reasons for not defining these small zones as separate cortical areas are dealt with in the Discussion.

A characteristic feature of the extrastriate cortex rostral to area 17 is the presence of bimodal units that respond to both visual and vibrissal stimulation. Bimodal units were recorded in the coarsely stippled region indicated in Figure 4A; those recorded closest to area 17 tended to have well-defined visual receptive fields and just barely detectable vibrissal responses. As the electrode penetrations progressed through the more rostral portion of this region toward somatosensory cortex (Woolsey, '67), vibrissal responses began to dominate and visual responses became less well defined. The coarsely stippled region that is lacking isoazimuth and isoelevation lines indicates an area in which bimodal units responded in a vigorous, well-defined manner to vibrissal stimulation while the visual response was weak and the visual receptive field diffuse and ill-defined.

In the lateral aspect of rostral extrastriate visual cortex, the visual representation is particularly distorted. This distortion is represented in Figure 4A by the nearly parallel placement of elevation and azimuth lines. A series of electrode penetrations proceeding for a considerable distance rostrally along the +20° isoelevation line would encounter receptive fields that were all near the 20° isoazimuth line. It is as though the nasal 30° of the visual field between 0° and +40° elevation were stretched in a direction parallel to the elevation lines, thereby providing a considerably expanded cortical representation of the nasal visual field; cortex in this area is also responsive to vibrissal stimulation throughout much of its extent.

Finally, there is another extrastriate visual region on the medial aspect of area 17 (Fig. 4A and B) that we have labelled Vm in keep-

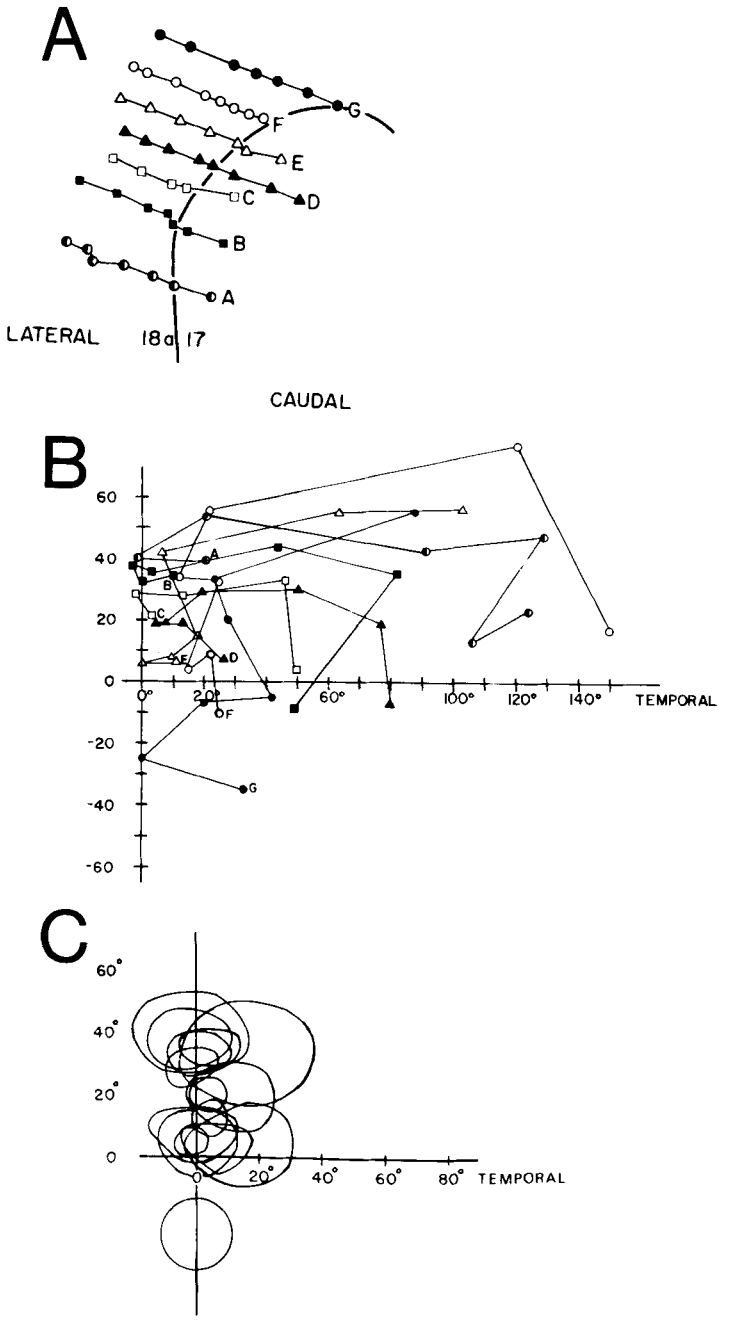

Fig. 7. Determination of the point of reversal in receptive field position along the rostro-lateral 17-18a border. A. A series of seven rows of electrode penetrations, each progressing from medial to lateral across the rostro-lateral extent of the 17-18a border. B. A plot of the receptive field positions obtained in the series of electrode penetrations shown in Figure 7A. The symbols indicate the center of the receptive field plotted at each electrode penetration; letters and symbols are the same as those used to indicate rows and penetrations in A. By following each set of symbols, it is evident that the point of reversal in receptive field position occurs in each case at or near the vertical meridian. Point to point comparisons between Figures 7A and B demonstrate that the reversal occurs at the 17-18a border. C. The most nasal receptive field encountered in each of the seven rows of electrode penetrations (A through G of Figure 7A) is plotted here to demonstrate that although receptive field centers are near the vertical meridian (0° azimuth), some of the receptive fields extend 10–20° into the ipsilateral visual field.

ing with the convention suggested for a similarly located region in the hamster (Tiao and Blakemore, '76). Vm corresponds to cytoarchitectonic area 18b (Caviness, '75). Responses to visual stimuli are more difficult to elicit in Vm than in other extrastriate regions, and it is therefore more difficult to define distinct receptive field boundaries. Nevertheless, it appears that the temporal visual field is represented twice in Vm (Fig. 4A and B) while the nasal 40° of the visual field is represented poorly, if at all. The two representations of the temporal visual fields are approximate mirror images of each other, although the caudal representation is larger than the rostral. We have, therefore, tentatively divided Vm into rostral and caudal subregions, Vm-r and Vm-c, on the basis of the retinotopic mapping data.

A summary of the retinotopic subdivisions of visual cortex and their relation to the cytoarchitectonic subdivisions described by Caviness ('75) is illustrated in Figure 8. The border of area 17 depicted by a solid line is that portion of the border that we have verified physiologically and have correlated with the cytoarchitectonics. The outermost borders of the extrastriate visual areas are represented as broken lines because we were unable to ascertain their absolute extent with certainty. As one records at greater distances from area 17, visual responses become less distinct and the receptive fields more diffuse, making it difficult at times to know the exact point where visual responses are no longer detectable. This is particularly true of the medial visual area. These lines may, however, be taken as delineating the approximate extent of visually responsive extrastriate cortex. Studies of cortico-cortical connections are currently underway in our laboratory to seek anatomical evidence for the subdivisions of lateral and medial extrastriate cortex described physiologically.

DISCUSSION

Subdivisions of visual cortex in the mouse

The retinotopic organization of the striate and extrastriate visual cortex in the mouse may be summarized as follows: 1) Striate visual cortex (area 17) contains one complete representation of the contralateral visual field, termed V1. 2) Cytoarchitectonic area 18a (Caviness, '75), which is lateral and rostral to area 17, contains at least two representations of the visual field. We propose that the more medial of these representations, which borders area 17 and has as its lateral border the +25° isoelevation line, be designated V2, and that the more lateral of these two representations be designated V3. 3) The visual field representations found medial to area 17 correspond to cytoarchitectonic area 18b (Caviness '75). Area 18b contains two representations of the temporal visual field that we have labelled Vm-r and Vm-c, and little or no representation of the most nasal aspect of the field.

The rationale for partitioning the lateral extrastriate cortex of the mouse in the manner outlined above derives from the description of the organization of the visual cortex in the monkey (Zeki, '69; Allman and Kaas, '71, '74a). In the owl monkey, V2 is a long narrow belt that extends around V1; the representation of the vertical meridian forms the border

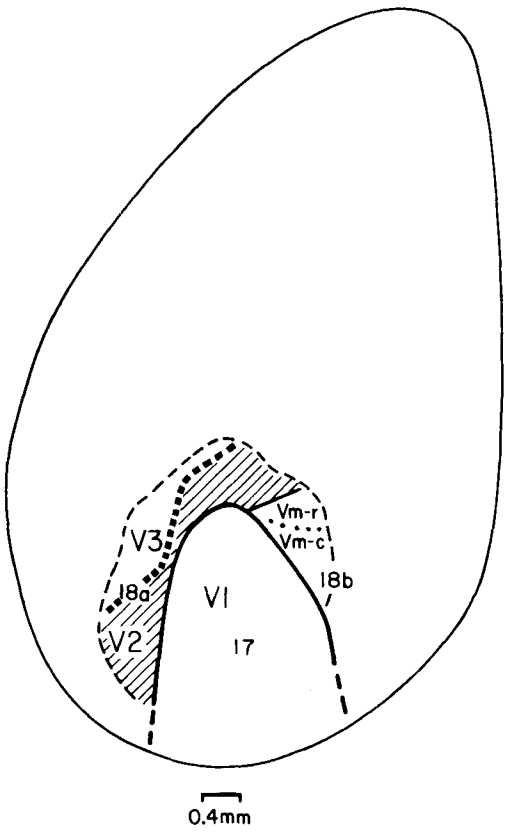

Fig. 8. Schematic dorsal view of the left hemisphere of the mouse, showing the relationship between the retinotopic subdivisions of visual cortex (V1, V2, V3, Vm) and the cytoarchitectonic subdivisions (areas 17, 18a, 18b).

between the two regions for much of its extent. The representation of the horizontal meridian bisects striate cortex and then extends across the width of the V2 belt, to divide V2 into a dorsal portion representing the lower visual field and a ventral portion representing the upper field. The horizontal meridian then bifurcates to form the outer boundary of these two subregions, which, taken together, yield a complete visual field representation that coincides with cytoarchitectonic area 18 (Allman and Kaas, '71, and '74a; Allman, '77). Although the observation that the part of area 17 that contains the representation of the horizontal meridian projects to two zones in area 18 was first made in the rhesus monkey (Cragg, '69; Zeki, '69), the complex convolutional pattern in this animal has made a complete description of its V2 more difficult (Van Essen and Zeki, '78).

Horizontal meridian

In attempting to subdivide the lateral extrastriate visual cortex of the mouse, we observed that the +25° isoelevation line appears to have the same role as the horizontal meridian in the owl monkey. In our map of the visual cortex of the mouse the medial border of V2 is easily defined as the 17-18a border, which includes a representation of the vertical meridian. The +25° isoelevation line, lying between the diverging isoelevation lines, nicely divides V2 into a rostral representation of the lower field and a caudal representation of the upper field. The +25° isoelevation line then trifurcates to form a convenient outer border for V2.

The apparent similarity between the +25° isoelevation line in the mouse and the horizontal meridian in the owl monkey in defining the outer border of V2 suggests that these two lines might have a similar position on the retina. Allman and Kaas ('71) defined the location of the horizontal meridian in the visual field of the owl monkey as a line perpendicular to the vertical meridian and passing through the projection of the optic disc, a definition justified by the fact that the center of the area centralis is on the same horizontal plane as the optic disc (Jones, '65). Although the mouse lacks an obvious area centralis (Chievitz, 1891), it is quite likely that it does have a central area of increased ganglion cell density, since no mammalian retina with a completely uniform ganglion cell density has thus far been described (Hughes, '77). The area of highest ganglion cell density in the retina of the rat is located temporal to and just above the optic disc (Fukuda, '77); its projection into the visual field would begin at about the same elevation as that of the optic disc and be centered at a point about 20° lower in the field. Since the projection of the optic disc of both the mouse (Drager, '78) and the rat (Hughes, '79) is located approximately 60° temporal to the midsaggital plane and 35° above the horizontal, it is reasonable to assume that the projection of the area of highest ganglion cell density in the mouse would be somewhat below this elevation as it is in the rat, thus suggesting that the +25° elevation line as defined in our experiments may be analogous to the horizontal meridian as defined in the experiments on the owl monkey. The position of the mouse's eye in the head supports this suggestion; a line drawn through the center of the pupil and perpendicular to it in an anesthetized mouse in our head holder forms a 25° angle above the horizontal, indicating that the optic axis is inclined about 25° upward. In addition, the 25° isoelevation line passes through the center of the expanded representation of the nasal visual field in area 17; such an area of expanded representation almost certainly is a reflection of a retinal area with a higher concentration of ganglion cells than the rest of the retina. Based on these indicators, we have labelled the +25° isoelevation line of Figure 4A as the "horizontal meridian" in the simplified representation in Figure 4B.

If one accepts the evidence that the +25° elevation line as defined in our experiments is analogous to the horizontal meridian, then V2 in the mouse is quite similar to V2 in the owl monkey. It is a narrow strip surrounding V1 on its lateral and rostral aspects; the vertical meridian forms a portion of its common border with V1, and the horizontal meridian forms its lateral border. The visual field representation in V2 is not a mirror image of that in V1; rather, the representation of the horizontal meridian splits to form the lateral border of V2 so that the upper and lower quadrants of the visual field are represented separately. As a consequence, adjacent points in the visual field on either side of the horizontal meridian are represented in separate parts of V2. V2 in the mouse therefore contains what Allman and Kaas ('74a) have termed a "second order transformation" of the visual field, just as it does in the owl monkey.

Information derived from studies of primates may or may not be an appropriate guide

for determining what further designations should be made lateral to the proposed V2 in the mouse. Primate extrastriate visual cortex is divisible into many more areas (Allman, '77; Van Essen, '78; Zeki, '76, '78) than are apparent in the mouse. In the owl monkey, there is an extensive series of partial representations of the visual field that comprise the third tier of extrastriate regions. In the mouse, the zone lateral to V2 that we have called V3 contains one more or less complete representation of the visual field anterolaterally, and an indication of a small representation of parts of the lower nasal field posteriorly (Fig. 4A). In addition, there is a small extra representation of part of the upper temporal visual field in the extreme posterolateral aspect of V2 (Fig. 4A) that we have included within V2 because it is medial to the representation of the horizontal meridian. It is possible that these small additional areas in V2 and V3 should be delineated as separate regions, perhaps forming a group similar to the third tier of the owl monkey. We have not done so in our schematic representations (Figures 4B and 8), primarily because the areas of cortex involved are too small to allow the number of electrode penetrations necessary to make such delineations with confidence.

Thalamic afferents

Area 18a of rodent extrastriate visual cortex receives its principal thalamic afferent innervation from the lateral posterior nucleus (Caviness and Frost, '80; Dursteler et al., '79; Hughes, '77; Robson and Hall, '77). The demonstration of a projection to 18a from the lateral geniculate nucleus in the rat (Hughes, '77) has not been confirmed in other rodents. In the mouse, thalamic afferents to 18a arise from the rostral aspect of the lateral posterior nucleus (LP_r) (Caviness and Frost, '80). The homologous thalamic nucleus in the grey squirrel, the rostral pulvinar, has been divided into lateral and medial subdivisions; rostrolateral pulvinar projects to area 18, while rostro-medial pulvinar projects to area 19, which adjoins area 18 laterally (Robson and Hall, '77). A demonstration of separate thalamic afferents to the medial and lateral aspects of area 18a in the mouse would lend support to our physiological subdivisions, but the small size of LPr and 18a has thus far precluded such an analysis.

The lateral nucleus (L) of the thalamus projects to area 18b in the mouse and hamster (Caviness and Frost, '80; Dursteler et al., '79). This projection arises in the caudal aspect of L in the mouse; lesions placed laterally in caudal L produce terminal degeneration in caudal 18b, while lesions invading both the medial and lateral aspects of caudal L produce degeneration in both rostral and caudal 18b (Caviness and Frost, '80). These findings suggest that there may be two subdivisions of caudal L, perhaps projecting to the two subregions of 18b that we have described.

Comparisons with other species

The observation that V2 in both the mouse and the monkey contains a split representation of the visual field, rather than a simple mirror image of the V1 representation, suggests that this organization may hold for other mammals as well. Montero et al. ('73b) indicated that there are five extrastriate visual areas in the albino rat. However, detailed visual field maps were not provided, making a direct comparison difficult. Two extrastriate visual areas were briefly described in a study of the visual cortex of the golden hamster (Tiao and Blakemore, '76). The medial visual area, called Vm, seems to correspond to area 18b in the mouse; as in the mouse, the area lateral to area 17 and contained within cytoarchitectonic area 18a was designated V2. In contrast to our findings in the mouse, V2 in the hamster was described as a mirror-image representation of V1, although the investigators indicated that this preliminary V2 map was based on the results of only a few electrode penetrations. From our experience in the mouse, a few penetrations would be sufficient to observe the reversal at the 17-18a border but would most likely miss the presence of a topographic discontinuity indicative of a split representation of the visual field. Two similar extrastriate visual regions have been described in the guinea pig, one lateral to V1 representing about 40° of the nasal visual field and one medial to V1 representing about 40° of the temporal field (Choudhury, '78). Although both regions were described as mirror images of the adjacent parts of V1, the author does not provide isoazimuth and isoelevation lines in the extrastriate regions to support this description. A more extensive study was carried out in the grey squirrel by Hall et al. ('71). In that study, both the V1-V2 and V2-V3 boundaries were identified on the basis of reversals of receptive field positions, and each visual area was considered to be a mirror image of the adjacent areas. However, in the absence of detailed maps of isoazimuth and

isoelevation lines for extrastriate visual cortex of the squirrel, the extent to which mouse and squirrel differ remains uncertain. The recent study of extrastriate regions in another rodent, *Octodon degus* (Olavarria and Mendez, '79) indicates two regions lateral to V1, and two others on the anterolateral and anteromedial borders of V1. Although the authors also do not provide maps with isoazimuth and isoelevation lines, their data may be interpreted to indicate that the region called LM immediately lateral to V1 is similar in many respects to V2 as we have outlined it in the mouse. The common border between V1 and LM in *Octodon degus* represents the vertical meridian; LM is a narrow strip in which the lower field is represented anteriorly and the upper field posteriorly. The horizontal meridian divides these two zones; since most of the points on the lateral border of LM (Olavarria and Mendez, '79: Fig. 1) represent the horizontal meridian, LM may also contain a split representation of the visual field.

Thompson et al. ('50) described the V2 representation of the rabbit as a mirror image of V1. However, the use of surface evoked potentials in that study may have obscured the fine details of the retinotopic map. Woolsey et al. ('73) recorded from unit clusters in the rabbit; in their preliminary report, they stated that the overall V2 map was similar to that described in the former investigation. They also reported finding at least one more extrastriate visual region, called AL (Anterolateral visual area) where visual, somatic, and auditory areas approach one another (Woolsey, et al., '73).

In a brief report of their study of the visual cortex of the cat, Bilge et al. ('67) were the first to show that the horizontal meridian forms the lateral boundary of V2, and thus that the visual field representation in V2 is split. The more extensive study of the extrastriate visual cortex of the cat carried out by Tusa et al. ('79) confirmed and extended this observation. They demonstrated that V2 is a long narrow band corresponding to area 18; the representation of the horizontal meridian lies along the caudal aspect of the border between V2 and V3 (area 19), but most of the rostral aspect of this border contains the representation of the far periphery of the visual field (Hubel and Wiesel, '65; Tusa et al., '79). In addition, there is apparently a considerable degree of variation in the visual field representation of the lower peripheral field in areas 18 and 19 from one cat to the next (Donaldson and Whitteridge, '77; Tusa et al., '79). Despite these complications, V2 in the cat is similar in many respects to V2 in the owl monkey: it is a narrow strip adjoining V1 that contains a split representation of the contralateral visual hemifield.

Our findings indicate that the organization of the V2 region of extrastriate visual cortex in the mouse resembles that outlined for the owl monkey and the cat. The similarity in the organization of V2 in these three distantly related mammals suggests that reinvestigation of other species may disclose more similarity to mouse, cat, and monkey than is currently evident.

ACKNOWLEDGMENTS

This work was supported by NIH Research grant R01-EY00621 from the National Eye Institute. E. Wagor and N.J. Mangini received support from NIH Training Grant T01-EY00092 from the National Eye Institute. We are grateful to Melba Miller for technical assistance.

LITERATURE CITED

Allman, J. (1977) Evolution of the visual system in the early primates. In: Progress in Psychobiology and Physiological Psychology, J. Sprague and A. Epstein, eds. Academic Press, New York, Vol. 7, pp. 1–53.

Allman, J.M., and J.H. Kaas (1971) A representation of the visual field in the caudal third of the middle temporal gyrus of the owl monkey *(Aotus trivirgatus)*. Brain Res. *31:*85–105.

Allman, J.M., and J.H. Kaas (1974a) The organization of the second visual area (VII) in the owl monkey: a second order transformation of the visual hemifield.Brain Res. 76:247–265.

Allman, J.M., and J.H. Kaas (1974b) A crescent-shaped cortical visual area surrounding the middle temporal area (MT) in the owl monkey *(Aotus trivirgatus)*. Brain Res. 81:199–213.

Allmann, J.M., and J.H. Kaas (1975) The dorsomedial cortical visual area: A third tier area in the occipital lobe of the owl monkey *(Aotus trivirgatus)*. Brain Res. *100:*473–487.

Allman, J.M., and J.H. Kaas (1976) Representation of the visual field on the medial wall of the occipital-parietal cortex in the owl monkey. Science *191:*572–575.

Benevento, L.A., and F.F. Ebner (1971) The areas and layers of corticocortical terminations in the visual cortex of the Virginia oppossum. J. Comp. Neurol. *141:*157–190.

Bilge, M., A. Bingle, K.N. Seneviratne, and D. Whitteridge (1967) A map of the visual cortex in the cat. J. Physiol. (London) 191:116P–118P.

Bishop, P.O., W. Kozak, and G.J. Vakkur (1962) Some quantitative aspects of the cat's eye: axis and plane of reference, visual field co-ordinates and optics. J. Physiol. *163:*466–502.

Brodmann, K. (1905) Beitrage zur histologischen Localisation der Grosshirnrinde. Dritte Mitteilung: Die Rinderfelder der niederen Affen. Leipzig: J. Psychol. Neurol. *4:*177–226.

Brodmann, K. (1909) Vergleichende Lokalisationslehre der Grosshirnrinde. Leipzig: J.A. Barth.

Caviness, V.S., Jr. (1975) Architectonic map of neocortex of the normal mouse. J. Comp. Neurol. *164:*247–263.

Caviness, V.S., and D.O. Frost. (1980) Thalamic projections to the neocortex in the mouse. II. Spatial order. J. Comp. Neurol. (in press).

Chievitz, J.H. (1891) Uber das Vorkommen der Area centralis retinae in den vier hoheren Wirbelthierklassen. Arch. Anat. Physiol. Anat. Abt. 311–334.

Choudhury, B.P. (1978) Retinotopic organization of the guinea pig's visual cortex. Brain Res. *144:*19–29.

Chow, K.K., A. Douville, G. Mascetti, and P. Grobstein (1977) Receptive field characteristics of neurons in a visual area of the rabbit temporal cortex. J. Comp. Neurol. *171:*135–146.

Cicerone, C.M., and D. Green (1977) Control of eye movements while recording from single units in the pigmented rat. Vision Res. *17:*985–987.

Cragg, B.G. (1969) The topography of the afferent projections in the circumstriate visual cortex of the monkey studied by the Nauta method. Vision Res. *9:*733–757.

De Vries, J. (1912) Uber die Zytoarchitektonik der Grosshirnrinde der Maus and uber die beziehungen der einzelnen Zellschichlen zum Corpus Callosum auf grund von experimentellen Lasionen. Folia Neurobiol. 6:288–322.

Donaldson, I.M.L., and D. Whitteridge (1977) The nature of the boundary between cortical visual areas II and III in the cat. Proc. R. Soc. Lond. B *199:*445–462.

Drager, U.C. (1975) Receptive fields of single cells and topography in mouse visual cortex. J. Comp. Neurol. *160:*269–290.

Drager, U.C. (1978) Observations on monocular deprivation in mice. J. Neurophysiol. *41:*28–42.

Droogleever Fortuyn, A.B. (1914) Cortical cell-lamination of the hemispheres of some rodents. Arch. Neurol. Psychiat. *6:*221–354.

Dursteler, M.R., C. Blakemore, and L.J. Garey (1979) Projections to the visual cortex in the golden hamster. J. Comp. Neurol. *183:*185–204.

Fraunfelder, F.T., and R.P. Burns (1970) Acute reversible lens opacity: caused by drugs, cold, anoxia, asphyxia, death and dehydration. Exp. Eye Res. *10:*19–30.

Fukuda, Y. (1977) A three group classification of rat retinal ganglion cells; histological and physiological studies. Brain Res. *119:*327–344.

Hall, W.C., J.H. Kaas, H. Killackey, and I.T. Diamond (1971) Cortical visual areas in the grey squirrel *(Sciurus carolinesis):* a correlation between cortical evoked potential maps and architectonic subdivisions. J. Neurophysiol. *34:*437–452.

Hubel, D.H., and T.N. Wiesel (1965) Receptive fields and functional architecture of two nonstriate visual areas (18 and 19) of the cat. J. Neurophysiol. *28:*229–289.

Hubel, D.H., and T.N. Wiesel (1970) Cells sensitive to binocular depth in area 18 of the macaque monkey cortex. Nature *225:*41–42.

Hughes, A. (1977) The topography of vision in mammals of contrasting life style: comparative optics and retinal organization. In: Handbook of Sensory Physiology, The Visual System in Vertebrates. F. Crescittelli, ed. Springer-Verlag, Berlin, Vol. VII/5, pp. 614–756.

Hughes, A. (1979) A schematic eye for the rat. Vision Res. *19:*569–588.

Hughes, H.C. (1977) Anatomical and neurobehavioral investigations concerning the thalamo-cortical organization of the rat's visual system. J. Comp. Neurol. *175:*311–336.

Isenschmid, R. (1911) Sur Kenntnis der Grosshirnrinde der Maus. Abh. Kon. Preuss. Akad. Wiss., Anhang. *3:*1–46.

Jones, A.E. (1965) The retinal structures of *(Aotus trivirgatus)* the owl monkey. J. Comp. Neurol. *125:*19–28.

Kaas, J.H. (1980) A comparative survey of visual cortex organization in mammals. In: Comparative Neurology of the Telencephalon, S. Ebbeson, ed. New York. Plenum Press.

Krieg, W.J.S. (1946a) Connections of the cerebral cortex. I. The Albino rat. A. Topography of cortical areas. J. Comp. Neurol. *84:*221–275.

Krieg, W.J.S. (1946b) Connections of the cerebral cortex. I. The albino rat. B. Structure of the cortical areas. J. Comp. Neurol. *84:*277–324.

Krieg, W.J.S. (1947) Connections of the cerebral cortex. I. The albino rat. C. Extrinsic connections. J. Comp. Neurol. *86:*267–394.

Mangini, N., and A.L. Pearlman (1980) Laminar distribution of receptive field properties in the primary visual cortex of the mouse, *Mus Musculus.* J. Comp. Neurol. *193:*203–222.

Mathers, L.H., A. Douville, and K.L. Chow (1977) Anatomical studies of a temporal visual area in the rabbit. J. Comp. Neurol. *171:*147–156.

Montero, V.M., H. Bravo, and V. Fernandez (1973a) Striate-peristriate cortico-cortical connections in the albino and grey rat. Brain Res. *53:*202–207.

Montero, V.M., and E.H. Murphy (1976) Corticocortical connections from the striate cortex in the rabbit. Anat. Rec. *184:*483.

Montero, V.M., A. Rojas, and F. Torrealba (1973b) Retinotopic organization of striate and peristriate visual cortex in the albino rat. Brain Res. *53:*197–201.

Olavarria, J., and B. Mendez (1979) The representations of the visual field on the posterior cortex of *Octodon degus.* Brain Res. *161:*539–543.

Palmer, L.A., A.C. Rosenquist, and R.J. Tusa (1978) The retinotopic organization of lateral suprasylvian visual areas in the cat. J. Comp. Neurol. *177:*237–256.

Pearlman, A.L., J. Birch, and J.C. Meadows (1979) Cerebral color blindness: an acquired defect in hue discrimination. Ann. Neurol. *5:*253–261.

Robson, J.A., and W.C. Hall (1977) The organization of the pulvinar in the grey squirrel *(Sciurus carolinensis).* II. Synaptic organization and comparisons with the dorsal lateral geniculate nucleus. J. Comp. Neurol. *173:*389–416.

Rose, M. (1912) Histologische Lokalisation der Grosshirnrinde bie Kleinen Saugetieren (Rodentia, Insectivora, Chiroptera). J. Psychol. Neurol. 19:389–479.

Rose, M. (1929) Cytoarchitektonischer Atlas der Grosshirnrinde der Maus. J. Psychol. Neurol. *40:*1–51.

Spatz, W.B., and J. Tigges (1972a) Experimental anatomical studies on the "middle temporal visual area (MT)" in primates. I. Efferent corticocortical connections in the marmoset *(Callithrix jacchus).* J. Comp. Neurol. *146:*451–463.

Spatz, W.B., and J. Tigges (1972b) Species difference between Old World and New World monkeys in the organization of the striate-prestriate association. Brain Res. *43:*591–594.

Thompson, J.M., C.N. Woolsey, and S.A. Talbot (1950) Visual areas I and II of cerebral cortex of rabbit. J. Neurophysiol. *13:*277–288.

Tiao, Y.-C., and C. Blakemore (1976) Functional organization in visual cortex of the golden hamster. J. Comp. Neurol. *168:*459–482.

Tigges, J., W.B. Spatz, and M. Tigges (1973) Reciprocal point-to-point connections between parastriate and striate cortex in the squirrel monkey *(Saimiri).* J. Comp. Neurol. *148:*481–490.

Tigges, J., W.B., Spatz, and M. Tigges (1974) Efferent cortico-cortical fiber connections of area 18 in the squirrel monkey *(Saimiri).* J. Comp. Neurol. *158:*219–236.

Towns, L.C., R.A. Giolli, and D.A. Haste (1977) Corticocortical fiber connections of the rabbit visual cortex: a fiber

degeneration study. J. Comp. Neurol. *173:*537–560.

Tusa, R.J., A.C. Rosenquist, and L.A. Palmer (1979) Retinotopic organization of areas 18 and 19 in the cat. J. Comp. Neurol. *185:*657–678.

Van Essen, D.C. (1979) Visual areas of the mammalian cerebral cortex. Ann. Rev. Neurosci. *2:*227–264.

Van Essen, D.C., and S.M. Zeki (1978) The topographic organization of rhesus monkey prestriate cortex. J. Physiol. *277:*193–226.

Woolsey, C.M., C. Sitti-Amorn, U.T. Keesey, and R.A. Holub (1973) Cortical visual areas of the rabbit. Soc. Neurosci. Abstr. *3:*180.

Woolsey, T.A. (1967) Somatosensory, auditory and visual cortical areas of the mouse. Johns Hopkins Med. J. *121:*91–112.

Zeki, S.M. (1969) Representation of central visual fields in prestriate cortex of monkey. Brain Res. *14:*271–291.

Zeki, S.M. (1971) Cortical projections from two prestriate areas in the monkey. Brain Res. *34:*19–35.

Zeki, S.M. (1976) The functional organization of projections from striate to prestriate visual cortex in the rhesus monkey. Cold Spring Harbor Symp. Quant. Biol. *40:*591–600.

Zeki, S.M. (1978) Uniformity and diveristy of structure and function in rhesus monkey prestriate visual cortex. J. Physiol. *277:*273–290.

Zeki, S.M., and D.R. Sandman (1976) Combined anatomical and electrophysiological studies on the boundary between the second and third visual areas of rhesus monkey cortex. Proc. R. Soc. Lond. Ser. B. *194:*555–562.